

Exchange effects in elastic collisions of spin-polarized electrons with open-shell molecules with $^3\Sigma_g^-$ symmetry

Motomichi Tashiro*

*Fukui Institute for Fundamental Chemistry, Kyoto University,
Takano-Nishi-Hiraki-cho 34-4, Kyoto 606-8103, Japan.*

(Dated: November 2, 2018)

Abstract

The spin-exchange effect in spin-polarized electron collisions with unpolarized open-shell molecules, O_2 , B_2 , S_2 and Si_2 , has been studied by the R-matrix method with the fixed-bond approximation. All of these molecules have $^3\Sigma_g^-$ symmetry in their ground states. Usual integrated cross sections with unpolarized electrons has also been studied. We used the complete active space self consistent field orbitals and put more than 10 target electronic states in the R-matrix models. In electron O_2 elastic collisions, calculated polarization fractions agree well with the experimental results, especially around the $^4\Sigma_u^-$ resonance. In e- B_2 , S_2 and Si_2 elastic collisions, larger spin-exchange effect is observed compared to the e- O_2 elastic collisions. In all four cases, spin-exchange effect becomes prominent near resonances. This association of resonance and magnitude of the spin-exchange effect was studied by explicitly removing the resonance configurations from the R-matrix calculations. In general, spin-exchange effect is larger in e- B_2 collisions than in e- S_2 and Si_2 collisions, and is smallest in e- O_2 collisions.

PACS numbers: 34.80.Bm, 34.80.Nz

*E-mail:tashiro@fukui.kyoto-u.ac.jp

I. INTRODUCTION

When electron collides elastically with open-shell atom or molecule, they can exchange their spins. Thus, spin polarization of the electron beam is in general reduced after scattering with unpolarized open-shell targets. We can obtain more precise information of the scattering process by studying this depolarization [1, 2, 3], which is difficult to observe in usual experiment with spin-averaging procedure.

Collisions of spin-polarized electrons with atoms have been studied for long years (see Hegemann et al.[4] and references therein). In contrast, number of experiment on electron molecule system is limited. Ratliff et al.[5] measured rate constants for electron exchange in elastic electron collisions with $O_2 X^3\Sigma_g^-$ and $NO X^2\Pi$ molecules in thermal energies. Their spin-exchange rate constants are substantially smaller than those in electron hydrogen-atom or alkali-metal-atom collisions. Hegemann et al.[1, 4] studied exchange process in elastic electron collisions with $O_2 X^3\Sigma_g^-$ and $NO X^2\Pi$ molecules and $Na 3^2S$ atoms. They measured ratio of spin-polarizations in electron beams before and after collisions, i.e., polarization fraction, which is directly related to the spin-exchange differential cross sections. As in the work of Ratliff et al.[5], Hegemann et al.[4] confirmed that the exchange cross sections of electron molecule collisions are much smaller than those of electron collisions with atoms. Although absolute value of spin-exchange cross section is small, the degree of spin-exchange in electron O_2 collisions becomes larger at 100 degrees with collision energies between 8 and 15 eV compared to the other angles and energies, which they attributed to the existence of the $O_2^- 4\Sigma_u^-$ resonance.

Theoretical study of spin-exchange in electron O_2 collisions was performed by da Paixao et al.[6]. They used the Schwinger multichannel method with the three lowest electronic states of O_2 in their model, and confirmed that spin-exchange cross section is small in electron $O_2 X^3\Sigma_g^-$ elastic scatterings. Although exchange cross sections are small for electron collisions with randomly oriented O_2 , they observed large depolarization at some scattering angles when electrons were scattered from spatially oriented O_2 molecules. The profile of depolarization as a function of scattering angle depends strongly on molecular orientation. Based on these results, da Paixao et al.[6] explained for the first time that the experimental exchange cross section in electron-molecule collisions is small because averaging over molecular orientation washes out depolarization effects. Fullerton et al.[7], Nordbeck et al.[8] and Wöste et al.[9] used the R-matrix method to calculate polarization fractions in electron O_2 collisions. The calculations of Fullerton et al.[7] and Nordbeck

et al.[8] employed the fixed bond approximation with T-matrix elements obtained by the nine-state R-matrix calculation of Noble and Burke [10], whereas Wöste et al.[9] used vibrational averaging of T-matrices to include the effect of nuclear motion. The fixed bond R-matrix calculations of Fullerton et al.[7] and Nordbeck et al.[8] confirmed the results of da Paixao et al.[6]. Agreement with experimental results at energies from 10 to 15 eV is marginal, as in the calculation of da Paixao et al.[6]. The vibrational averaging procedure of Wöste et al.[9] improved agreement with the experimental results in this energy region. Machado et al.[11] applied the Schwinger variational iterative method combined with the distorted-wave approximation and obtained similar elastic e-O₂ polarization fractions to those of Fullerton et al.[7].

Other than electron O₂ collisions, theoretical work of spin exchange in electron molecule collisions is scarce. da Paixao et al.[12] calculated polarization fractions in electron NO X²Π elastic collisions as they did in electron O₂ collisions [6]. Calculated exchange effect was small in e-NO elastic collisions, in agreement with the experimental results of Hegemann et al.[1, 4]. Sartori et al.[13] studied spin-exchange in the superelastic electron collisions with H₂ c ³Π_u state using the Schwinger multichannel method. Large depolarization was observed in their results, intermediate between depolarizations in e-Na and e-O₂ collisions. Recently, Fujimoto et al.[14] performed the iterative Schwinger variational calculation of spin-exchange effect in elastic electron C₂O X³Σ⁻ collisions. They found modest depolarization near resonances, however, spin-exchange effect was very small in other energy region.

Recently, we have studied electron O₂ scatterings by the R-matrix method with improved molecular orbitals and increased number of target states[15, 16] compared to the previous theoretical studies. Our results are in good agreement with the previous experimental results. Since the previous theoretical polarization fractions of elastic e-O₂ collisions at energies between 10 and 15eV agree not so well with the experimental results, it would be interesting to examine how spin-exchange cross section will change in this energy region by our improved calculational parameters. At the same time, it is important to understand general behaviour of spin-exchange cross sections, polarization fractions in other words, in elastic electron molecule collisions. Until now, spin-exchange effect in low-energy electron molecule elastic scattering has been studied only for NO and C₂O molecules other than O₂. Thus it is desirable to study spin-exchange in other electron-molecule scattering systems as well. In this work, we study spin-exchange in electron O₂ collisions with the same calculational parameters as we used in our previous works[15, 16]. In addition, we calculate spin-exchange cross section in elastic electron collisions with B₂, S₂ and Si₂

molecules. These B₂, S₂ and Si₂ are stable homo-nuclear molecules with $^3\Sigma_g^-$ symmetry in their ground states, as in O₂ molecule.

In this paper, details of the calculations are presented in section 2, and we discuss the results in section 3 comparing our results with previous theoretical and available experiments. Then the summary is given in section 4.

II. THEORETICAL METHODS

A. polarization fraction

In this work, we consider elastic scattering of spin-polarized electrons from randomly oriented unpolarized molecules. When the incident electrons have spin polarization P and the scattered electrons have polarization P' , with the polarization direction perpendicular to the scattering plane, the polarization fraction, the ratio of P and P' , is a measure of spin-exchange and is related to the spin-flip differential cross section (DCS) $d\sigma_{\text{SF}}/d\Omega$ as [1, 7],

$$\frac{P'}{P} = 1 - 2 \frac{d\sigma_{\text{SF}}/d\Omega}{d\sigma/d\Omega}. \quad (1)$$

Here $d\sigma/d\Omega$ is the DCS obtained by unpolarized electrons.

The DCSs of $d\sigma/d\Omega$ and $d\sigma_{\text{SF}}/d\Omega$ are evaluated by the spin-specific scattering amplitude [7, 16],

$$f_{ij}^S = \sum_{l_i m_i l_j m_j} \sum_{\Gamma \lambda \mu \nu} \frac{\sqrt{\pi(2l_i+1)}}{\sqrt{k_i k_j}} i^{l_i-l_j+1} \mathcal{D}_{0\lambda}^{l_i*}(\alpha\beta\gamma) \mathcal{D}_{\nu\mu}^{l_j}(\alpha\beta\gamma) Y_{l_j}^{\nu}(\hat{r}) C_{\lambda m_i} C_{\mu m_j}^* T_{ij}^{\Gamma S M_S}, \quad (2)$$

where i and j specify the states of the target molecule as well as the scattering electron in the initial and final channels, respectively. k_i and k_j are the initial and final wavenumber of the electron, $\mathcal{D}_{m m'}^l(\alpha\beta\gamma)$ is the rotation matrix with the Euler angles (α, β, γ) representing orientation of the target molecule in the laboratory frame. The electron is scattered to the direction \hat{r} in the laboratory frame in this expression. The T-matrix elements $T_{ij}^{\Gamma S M_S}$ are prepared for all possible spin S of the electron-molecule system as well as all irreducible representation Γ of the symmetry of the system. We used D_{2h} in the R-matrix calculations. Since the target molecules have triplet spin symmetry in this work, we only include $S = 1/2$ and $3/2$ in our calculations. The matrix element $C_{\lambda m}$ relates the spherical harmonics Y_l^λ to the real spherical harmonics S_l^m . The explicit expression of $C_{\lambda m}$ can be found in our previous paper [16].

In this paper, we consider elastic scattering of electron from molecule with triplet spin symmetry. Then, $d\sigma/d\Omega$ and $d\sigma_{\text{SF}}/d\Omega$ are expressed by the spin specific amplitude f^S as [1, 7],

$$\frac{d\sigma}{d\Omega} = \frac{1}{3} \left(2 |f^{3/2}|^2 + |f^{1/2}|^2 \right), \quad (3)$$

and

$$\frac{d\sigma_{\text{SF}}}{d\Omega} = \frac{4}{27} |f^{3/2} - f^{1/2}|^2. \quad (4)$$

Here summations over channel indices are omitted for notational simplicity. Note that the expression of the spin-flip DCS contains interference of amplitudes with different spin multiplicities. Since the target molecules are randomly oriented, these DCSs are averaged over all possible molecular orientations in space.

B. Detail of the R-matrix calculation

The T-matrix elements $T_{ij}^{\Gamma S M_s}$ were obtained by a modified version of the polyatomic programs in the UK molecular R-matrix codes [17]. General procedure of calculation is almost the same as in our previous works[15, 16]. Since the R-matrix method itself has been described extensively in the literature [17, 18, 19] and references therein, we do not repeat general explanation of the method here.

In this work, elastic electron collisions with O_2 , B_2 , S_2 and Si_2 molecules were studied. For electron O_2 scattering, we used the same parameter set as we used in the previous works[15, 16]. Specifically, we employed the equilibrium bond length of $2.300 a_0$ for O_2 , the R matrix radius of $10 a_0$. The angular quantum number of the scattering electron was included up to $l=5$. The atomic basis set for bound molecular orbitals, number of the target states included in the model as well as choice of the configurations in the inner region calculation were the same.

For the electron B_2 , S_2 and Si_2 scatterings, we included 14, 13 and 15 target electronic states in the R-matrix calculation, respectively. Symmetries and spin-multiplicities of these states are given in table I. These target states were represented by valence configuration interaction wave functions constructed by the state averaged complete active space SCF (SA-CASSCF) orbitals. Fixed-bond approximation was employed with internuclear distances of 3.036 , 3.700 and $4.400 a_0$ for B_2 , S_2 and Si_2 , respectively. Although we study only elastic scattering in this work, we included these excited target states to improve quality of the R-matrix calculations. Also, by including these excited states, we can suppress artificial structure coming from pseudo-resonance. In this study,

the SA-CASSCF orbitals were obtained by calculations with MOLPRO suites of programs [20]. The target orbitals of B_2 , S_2 and Si_2 were constructed from the cc-pVTZ basis set [21, 22]. The radius of the R-matrix sphere was chosen to be $13 a_0$, which is larger than the R-matrix sphere used in the electron O_2 calculation. We need this extended R-matrix sphere to avoid overlap of B_2 , S_2 and Si_2 molecular orbitals with the R-matrix boundary. In order to represent the scattering electron, we included diffuse gaussian functions up to $l = 4$, with 13 functions for $l = 0$, 11 functions for $l = 1$, 10 functions for $l = 2$, 8 functions for $l = 3$, 6 functions for $l = 4$. Exponents of these diffuse gaussians were taken from Faure et al. [23]. The construction of the configuration state functions (CSFs) for the electron-molecule system is the same as in our previous e- O_2 papers [15, 16]. Two different kind of $(N + 1)$ -electron configurations are included, where N is a number of electrons in the target molecule. The first type of the $(N + 1)$ -electron CSFs is constructed from N target molecular orbitals (MOs) plus one continuum orbital. The second type of CSFs is constructed from the $N + 1$ target MOs. These target MOs are just the SA-CASSCF orbitals, whereas the continuum orbitals are obtained by orthogonalization of the diffuse gaussian functions to the target MOs [17]. Since only the continuum orbitals have overlap with the R-matrix sphere, the first type of CSFs mainly contributes the cross sections. However, the second type of CSFs is also important, as it is crucial to describe resonance. For reference, we show orbital set used in the e- B_2 calculation in table II. The orbital sets for e- S_2 and e- Si_2 scatterings are very similar. More detailed explanation can be found in our previous paper [15].

III. RESULTS AND DISCUSSION

A. Excitation energies

In this section, we show excited state energies of B_2 , S_2 and Si_2 molecules. Since O_2 energies have been shown in our previous paper [15], we do not discuss them here. In table III, calculated excitation energies of B_2 molecule are compared with full configuration interaction (FCI) vertical excitation energies of Hald et al. [24]. Although they employed different basis set, aug-cc-pVDZ, and shorter internuclear distance of $3.005 a_0$, our CASSCF values agree reasonably well with their results. In table IV, our CASSCF energies of S_2 molecule are compared with MRD CI vertical excitation energies of Hess et al. [25] and MRCI adiabatic excitation energies of Kiljunen et al. [26]. In this case, our results agree well with the previous calculations for the lowest two excitations. For

excitation energies to the three higher states, deviations become larger because Kiljunen et al.[26] studied adiabatic excitation energies whereas we calculated vertical excitation energies. In table V, calculated energies of Si₂ molecule are compared with MRD CI vertical excitation energies of Peyerimhoff and Buenker [27]. Since they employed shorter internuclear distance of 4.3 a₀ compared to 4.4 a₀ of our calculation, precise comparison is difficult. However, our CASSCF results agree reasonably well with their results.

B. Integral cross sections

In figure 1 (a), integral cross sections (ICSs) for elastic electron collision with O₂ molecules are shown. The sharp peak around 0.2 eV comes from the O₂⁻ 2Π_g resonance. Also, 4Σ_u⁻ resonance causes a small rise of cross section around 13eV. The details of these e-O₂ ICSs were discussed in the previous paper[15], however, they are shown here for comparison with the ICSs of the electron B₂, S₂ and Si₂ collisions.

In figure 1 (b), elastic ICSs for electron B₂ collisions are shown. In this case, very large cross section is observed near zero energy, about 10⁻¹⁴cm², compared to 10⁻¹⁶cm² in the e-O₂ collisions. The partial cross sections of 2Σ_g⁻ and 4Σ_g⁻ symmetries equally contribute to this enhancement. There is a broad peak around 3 eV, which comes from 4Π_g symmetry partial cross section. An analysis of configuration state functions (CSFs) suggests that this peak is related to the configuration (1σ_g)²(1σ_u)²(2σ_g)²(2σ_u)²(1π_u)²(1π_g)¹, which is the ground state B₂ with a scattering electron attached to the 1π orbital. By removing this (1π_g)¹ configuration from the R-matrix calculation, this peak vanishes from the ICSs.

In figure 2 (a), ICSs for elastic electron scattering with S₂ molecules are shown. The magnitude of the ICS increases from 2.0 × 10⁻¹⁵ at zero energy to 3.5 × 10⁻¹⁵cm² at 10 eV, then it decreases to 3.0 × 10⁻¹⁵cm² at 15 eV. Although the magnitudes are different, the profiles of the 2Σ_g⁻ and 4Σ_g⁻ symmetry partial cross sections are very similar to those partial cross sections in the e-O₂ elastic collision. A broad peak is observed around 4.5 eV, which comes from the 4Σ_u⁻ symmetry partial cross section. The CSF analysis suggests that this peak is related to the configuration (core)²⁰(4σ_g)²(4σ_u)²(5σ_g)²(2π_u)⁴(2π_g)²(5σ_u)¹, and likely belongs to the S₂⁻ 4Σ_u⁻ resonance. The 2Σ_u⁻ symmetry partial cross section has also a small rise around 6 eV (not shown in the figure), its contribution to the total ICS is small. Two anomalous structures are observed in the ICS, a kink at 2.7 eV and a cusp at 5 eV. The former kink belongs to the 2Π_u partial cross section, whereas

The cusp at 5 eV comes from the $^4\Sigma_u^-$ symmetry. We analyzed the CSFs and found that the kink at 2.7 eV is likely related to a resonance with configuration $(\text{core})^{20}(4\sigma_g)^2(4\sigma_u)^2(5\sigma_g)^2(2\pi_u)^3(2\pi_g)^4$, which is obtained from an attachment of the scattering electron to the excited $c^1\Sigma_u^-$, $A^3\Delta_u$ and $A^3\Sigma_u^+$ states of S_2 with configuration $(\text{core})^{20}(4\sigma_g)^2(4\sigma_u)^2(5\sigma_g)^2(2\pi_u)^3(2\pi_g)^3$. The position of the cusp coincides with the S_2 $B^3\Sigma_u^-$ state, thus it is associated with opening of this excitation channel.

In figure 2 (b), ICSs for elastic electron scattering with Si_2 molecules are shown. The magnitude of the ICS is about $3.0 - 5.0 \times 10^{-15} \text{cm}^2$ between 0 and 15 eV. There are two sharp peaks below 1 eV. The peak at 0.55 eV is from the $^2\Pi_g$ symmetry partial cross sections and the other peak at 0.12 eV is from the $^4\Pi_g$ symmetry. We checked the CSFs of the $^2\Pi_g$ and $^4\Pi_g$ symmetry calculations and found that the configuration $(\text{core})^{20}(4\sigma_g)^2(4\sigma_u)^2(5\sigma_g)^2(2\pi_u)^2(2\pi_g)^1$ has dominant contribution to these resonances.

C. Polarization fractions

In figure 3, calculated polarization fractions (PFs) for elastic electron O_2 collisions are shown for scattering energies of 5, 10, 12 and 15 eV with the previous theoretical results of Fullerton et al.[7], Machado et al.[11], da Paixão et al.[6] and Wöste et al.[9]. These theoretical results are also compared with the experimental values of Hegemann et al.[1] in the figure. As we can see from eq.1, deviation of PF from unity is a measure of spin-exchange. Our e- O_2 PFs are close to 1 at all scattering energies, indicating the degree of spin-exchange is relatively small. For 5 eV, our results are very similar to the previous R-matrix results of Fullerton et al.[7]. The results of Machado et al.[11] are also similar, but smaller at low angles below 30 degrees. Our PFs at 10eV are slightly smaller than the results of Fullerton et al.[7] and Machado et al.[11]. The PFs of da Paixao et al.[6] at 10 eV are smaller than our results in all angles, especially 120-180 degrees. Our calculation cannot reproduce the drop of experimental PFs at 10 eV at 100 degrees. The PFs of Wöste et al.[9] have a minimum at this position and their value at 100 degree is the closest to the experimental result, although there is still some deviation in magnitude. At collision energy of 12 eV, the results of our calculation, Wöste et al.[9] and Fullerton et al.[7] have similar angular behaviour, though our results are smaller than the others at all angles. All of these three theoretical results agree reasonably well with the experimental results. For 15eV, our PFs are larger than the results of the other theoretical calculations in all scattering angles and are closer to the experimental results. The PFs of Fullerton et al.[7] and Machado et al.[11] are very similar

in shape and magnitude, whereas the results of da Paixao et al.[6] are slightly smaller at higher angles above 110 degrees. The deviation of our PFs from the previous theoretical results is the largest around 90-110 degrees, where there is a dip in the profile. Although the magnitude of the PFs are different, the shape of the our PF profiles itself is similar to the previous calculations.

In figure 4, the PFs for elastic electron O₂ collisions are shown as a function of energy at a scattering angle of 100 degrees. Our result has a minimum at 13 eV, however, it is located at 15 eV and 12 eV in the result of Fullerton et al.[7] and Wöste et al.[9], respectively. The magnitude of the PF at the minimum is larger in Wöste et al.[9] than in our calculation and Fullerton et al.[7].

For comparison of the e-O₂ PFs with the PFs of electron B₂, S₂ and Si₂ collisions in the following figures, the PFs of elastic electron O₂ collisions are again shown in the figure 5 (a) for collision energies of 3, 5, 7, 10 and 15 eV. The depolarization, i.e., deviation of PF from 1, is only prominent at 10 and 15 eV where the $^4\Sigma_u^-$ resonance exists as shown in fig.1 (a). In order to check the relation of the $^4\Sigma_u^-$ resonance and the PFs at 15 eV, we have carried out the R-matrix calculation with modified configurations, removing the $(1\sigma_g)^2(1\sigma_u)^2(2\sigma_g)^2(2\sigma_u)^2(3\sigma_g)^2(1\pi_u)^4(1\pi_g)^2(3\sigma_u)^1$ configuration from the original calculation. By this procedure we can suppress the effect of the resonance. The results in the fig. 5 (a) indicates that the PFs become very close to 1 by removing the configuration of the $^4\Sigma_u^-$ resonance.

In figure 5 (b), calculated PFs for elastic electron B₂ collisions are shown for scattering energies of 3, 5, 7, 10 and 15 eV. For most of the scattering energies and angles, the depolarization in electron B₂ collision is larger than that in electron O₂ collisions. Between 80 and 180 degrees, the magnitude of the PFs are about 0.8-0.9 at all energies. In contrast, the e-O₂ PFs are larger than 0.9. The e-B₂ PFs show large depolarization effect at scattering energies of 3 and 5 eV, which are close to the $^4\Pi_g$ resonance. In order to understand the origin of the large depolarizations at 3 and 5 eV, we excluded the effect of the B₂⁻ $^4\Pi_g$ resonance around 3.5 eV and re-calculated the e-B₂ PFs. Specifically, we removed $(1\sigma_g)^2(1\sigma_u)^2(2\sigma_g)^2(2\sigma_u)^2(1\pi_u)^2(1\pi_g)^1$ configuration from the R-matrix calculation and erased the $^4\Pi_g$ resonance. As shown in the fig. 5 (b), the effect of the resonance on the PFs is evident. With the resonance effect, the lowest value of the PF at 3 eV is about 0.7 at 90 degrees, but it becomes about 0.95 without the resonance contribution. Also, the depolarizations at 5 and 7 eV become less pronounced when we remove the effect of the resonance.

The calculated PFs for elastic electron S₂ collisions are shown in figure 6 (a). In general, the degree of depolarization is smaller than the e-B₂ case, but is larger than the e-O₂ case. The profiles of the PFs at 7, 10 and 15 eV look similar to each other. However, the PFs at 3 and 5 eV behave

differently. The degree of depolarization is larger at forward angles for 3 eV case, however, it is larger at backward angles at 5 eV. To understand the effect of resonance on electron S_2 PFs, we removed the $(\text{core})^{20}(4\sigma_g)^2(4\sigma_u)^2(5\sigma_g)^2(2\pi_u)^4(2\pi_g)^2(5\sigma_u)^1$ configuration and erased the $^4\Sigma_u^-$ resonance at 4.5eV, then re-calculated the PFs. The results are shown in the same figure. As in the case of electron B_2 PFs, the degree of depolarization becomes smaller when we removed the resonance effect.

The calculated PFs for elastic electron Si_2 collisions are shown in figure 6 (b). In this case, relatively large depolarization is observed for 3 eV at 100 degrees. The depolarization becomes smaller as the collision energy increases, however, some degree of depolarization remains near 80 and 180 degrees. The effect of resonance on the electron Si_2 PFs were examined by removing the $(\text{core})^{20}(4\sigma_g)^2(4\sigma_u)^2(5\sigma_g)^2(2\pi_u)^2(2\pi_g)^1$ configuration, which is responsible for the $^2\Pi_g$ and $^4\Pi_g$ resonances at 0.12 and 0.55 eV, respectively. By removing this configuration, these two sharp peaks in the ICSs disappear. The PFs without the resonances are shown in the fig. 6 (b). For 3 eV case, the depolarization becomes smaller at all angles. However, the decrease of depolarization is not so large compared to the cases of e- B_2 and e- S_2 collisions. For 5 eV case, the depolarization at 85 degrees becomes larger, though it becomes smaller at backward angles. Thus, in this case, the association of the resonances with the depolarization is not so straightforward as in the e- O_2 , B_2 and S_2 cases.

D. Discussion

As we show in the figures 5 and 6, existence of resonance and behaviour of PF is closely related each other. When resonance exists at some energy, relatively large depolarization is observed compared to the other energies. Also, when the resonance is artificially removed by deleting specific configuration in the R-matrix calculation, depolarization becomes smaller in general. In case of electron Si_2 collisions, this trend is partly broken at 5 eV around 80 degrees, however, depolarization generally becomes smaller at the other region after removing the resonance effect. The association of resonance and PF has been discussed in the previous theoretical and experimental papers [1, 7, 9], and we have confirmed this association more clearly by explicitly studying the effect of resonance on the PF of four different electron-molecule systems.

Even if collision occurs away from the resonance energy, some degree of depolarization is observed in all cases of e- O_2 , B_2 , S_2 and Si_2 collisions. In e- B_2 case, depolarization is relatively

large even outside of the resonance energy region. In contrast, the PFs in e-O₂ collisions are very close to 1 when collision energy is distant from the resonance energy. The degree of depolarization in e-S₂ and Si₂ collisions is intermediate between e-B₂ and e-O₂ depolarizations. It is unclear why different degree of depolarization is seen in these four electron-molecule collisions when collision energy is distant from resonance. The extent of molecular orbitals may be related to this difference, as discussed by Sartori et al.[13] on the electron H₂ superelastic collisions.

For the electron O₂ elastic scattering, the previous theoretical and experimental PFs are available for comparison with our results. Our low energy PFs at 5 and 10 eV are similar to the other theoretical results. However, the PFs at 12eV are smaller than the previous results at all angles, and our PFs at 15eV are much closer to unity than the other theoretical results as shown in fig.3. The reason of these deviations can be attributed to the shift of O₂⁻ ⁴Σ_u⁻ resonance position. In our calculation, the position of the ⁴Σ_u⁻ resonance peak is located around 13.0 eV, whereas it is around 14.1 eV in the previous R-matrix calculation. As discussed in Wöste et al.[9], the position of the ⁴Σ_u⁻ resonance is sensitive to the internuclear distance. In this work, the internuclear length is fixed to be 2.3 a₀ and it is the same as in the calculation of Fullerton et al.[7]. So the choice of basis set, molecular orbitals and number of target states is important to the difference in the position of the resonance. Probably the position of resonance is stabilized by inclusion of more target states in the present R-matrix calculations compared to the previous calculations of Fullerton et al.[7], Machado et al.[11] and da Paixão et al.[6].

In figure 1 (b), sharp increase of cross section is observed in electron B₂ elastic scattering near zero energy. This increase of cross section is similar to the case of electron polar-molecule collision, although B₂ molecule has no dipole moment. The cross section of electron CO₂ elastic collision also has similar sharp increase near zero energy, and several experimental and theoretical works have been performed to understand this behaviour. Morrison analyzed this problem and suggested that this behaviour is related to the existence of a virtual state [28]. Morgan has shown that the correlation and polarization effect is important for this sharp peak [29]. Similar mechanism may exist for the electron B₂ elastic collisions.

For the electron O₂ elastic collisions, we put larger number of target electronic states and better quality molecular orbitals in the R-matrix calculations, and obtained improved results around ⁴Σ_u⁻ resonance region compared to the previous fixed-bond calculations. However, the results of Wöste et al.[9] agree better with the experimental PFs at 10 eV. They achieved this good agreement by vibrational averaging of the T-matrices to include the effect of the nuclear motion. By extend-

ing the present R-matrix calculation to include the vibrational effect using vibrational averaging procedure or the non-adiabatic R-matrix method, we may obtain better agreement with the experimental PFs. Also, inclusion of nuclear motion effect may improve the quality of the calculations on electron B₂, S₂ and Si₂ elastic collisions.

IV. SUMMARY

We have calculated the polarization fractions (PFs) on low-energy elastic collisions of spin-polarized electrons with open-shell molecules, O₂, B₂, S₂ and Si₂, all of them having $^3\Sigma_g^-$ symmetry in their ground states. As in our previous works, we employed the fixed-bond R-matrix method based on state-averaged complete active space SCF orbitals. Our PFs for electron O₂ collisions agree better with the previous experimental result, especially around the $^4\Sigma_u^-$ resonance, compared to the previous theoretical calculations. Larger spin-exchange effect is observed in the electron B₂ and Si₂ collisions than in the e-O₂ collisions. In e-S₂ collisions, degree of depolarization is similar to the e-O₂ collisions. In all four electron-molecule collisions, the PFs deviate larger from 1 near resonances. This association of resonance and PF was explicitly confirmed by the R-matrix calculations removing configurations responsible for the resonance.

-
- [1] T. Hegemann, S. Schroll, and G. F. Hanne, *J. Phys. B* **26**, 4607 (1993).
 - [2] K.-N. Huang, *Chinese Journal of Physics* **25**, 156 (1987).
 - [3] K. Bartschat and D. H. Madison, *J. Phys. B* **21**, 2621 (1988).
 - [4] T. Hegemann, M. Oberste-Vorth, R. Vogts, and G. F. Hanne, *Phys. Rev. Lett.* **66**, 2968 (1991).
 - [5] J. M. Ratliff, G. H. Rutherford, F. B. Dunning, and G. K. Walters, *Phys. Rev. A* **39**, 5584 (1989).
 - [6] F. J. da Paixão, M. A. P. Lima, and V. McKoy, *Phys. Rev. Lett.* **68**, 1698 (1992).
 - [7] C. M. Fullerton, G. Wöste, D. G. Thompson, K. Blum, and C. J. Noble, *J. Phys. B* **27**, 185 (1994).
 - [8] R.-P. Nordbeck, C. M. Fullerton, G. Wöste, D. G. Thompson, and K. Blum, *J. Phys. B* **27**, 5375 (1994).
 - [9] G. Wöste, K. Higgins, P. Duddy, C. M. Fullerton, and D. G. Thompson, *J. Phys. B* **29**, 2553 (1996).
 - [10] C. J. Noble and P. G. Burke, *Phys. Rev. Lett.* **68**, 2011 (1992).
 - [11] L. E. Machado, E. M. S. Ribeiro, M.-T. Lee, M. M. Fujimoto, and L. M. Brescansin, *Phys. Rev. A* **60**,

- 1199 (1999).
- [12] F. J. da Paixão, M. A. P. Lima, and V. McKoy, *Phys. Rev. A* **53**, 1400 (1996).
 - [13] C. S. Sartori, F. J. da Paixão, and M. A. P. Lima, *Phys. Rev. A* **55**, 3243 (1997).
 - [14] M. M. Fujimoto, S. E. Michelin, I. Iga, and M.-T. Lee, *Phys. Rev. A* **73**, 012714 (2006).
 - [15] M. Tashiro, K. Morokuma, and J. Tennyson, *Phys. Rev. A* **73**, 052707 (2006).
 - [16] M. Tashiro, K. Morokuma, and J. Tennyson, *Phys. Rev. A* **74**, 022706 (2006).
 - [17] L. A. Morgan, J. Tennyson, and C. J. Gillan, *Comput. Phys. Commun.* **114**, 120 (1998).
 - [18] P. G. Burke and J. Tennyson, *Mol. Phys.* **103**, 2537 (2005).
 - [19] J. D. Gorfinkiel, A. Faure, S. Taioli, C. Piccarreta, G. Halmova, and J. Tennyson, *Eur. Phys. J. D* **35**, 231 (2005).
 - [20] H.-J. Werner, P. J. Knowles, R. Lindh, M. Schütz, et al., *Molpro version 2002.6, a package of ab initio programs*.
 - [21] T. H. Dunning, Jr., *J. Chem. Phys.* **90**, 1007 (1989).
 - [22] D. E. Woon and T. H. Dunning, Jr., *J. Chem. Phys.* **98**, 1358 (1993).
 - [23] A. Faure, J. D. Gorfinkiel, L. A. Morgan, and J. Tennyson, *Comput. Phys. Commun.* **144**, 224 (2002).
 - [24] K. Hald, P. Jørgensen, J. Olsen, and M. Jaszuński, *J. Chem. Phys.* **115**, 671 (2001).
 - [25] B. Hess, R. J. Buenker, C. M. Marian, and S. D. Peyerimhoff, *Chem. Phys.* **71**, 79 (1982).
 - [26] T. Kiljunen, J. Eloranta, H. Kunttu, L. Khriachtchev, M. Pettersson, and M. Räsänen, *J. Chem. Phys.* **112**, 7475 (2000).
 - [27] S. D. Peyerimhoff and R. J. Buenker, *Chem. Phys.* **72**, 111 (1982).
 - [28] M. A. Morrison, *Phys. Rev. A* **25**, 1445 (1982).
 - [29] L. A. Morgan, *Phys. Rev. Lett.* **80**, 1873 (1998).

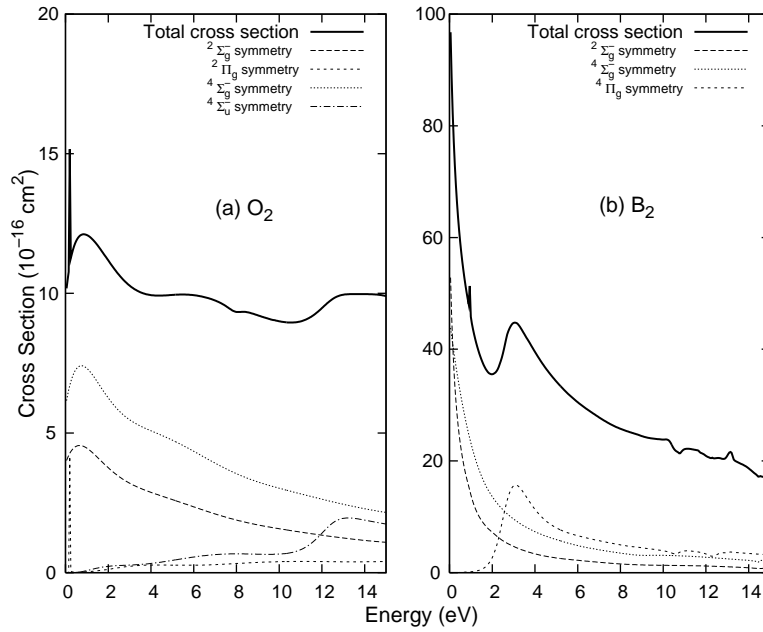


FIG. 1: Panel (a): the elastic integrated cross sections (ICSs) of electron scattering by O_2 molecules. Panel (b): the elastic ICSs of electron scattering by B_2 molecules. Thick full lines represent total cross sections. The partial cross sections are represented by thin lines. Symmetries with minor contributions are not shown in the figure.

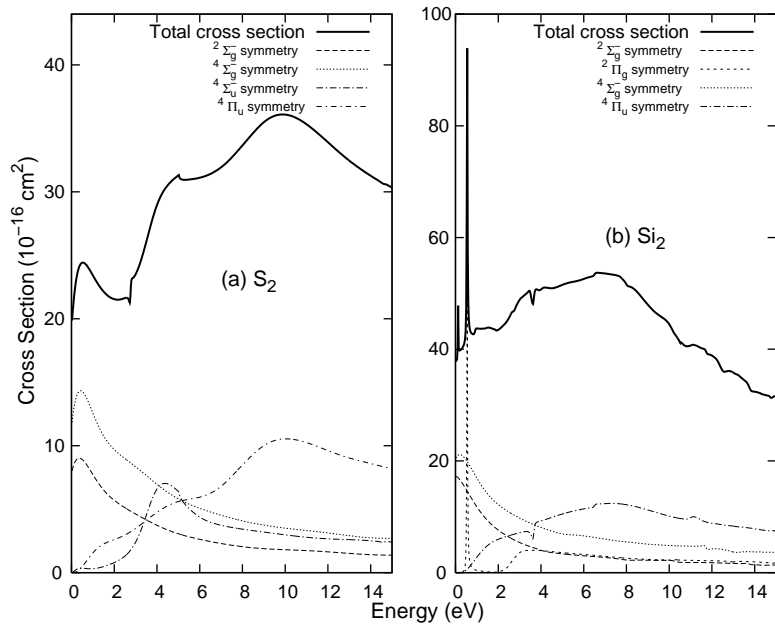


FIG. 2: Panel (a): the elastic ICSs of electron scattering by S_2 molecules. Panel (b): the elastic ICSs of electron scattering by Si_2 molecules. Other details are the same as in the figure 1.

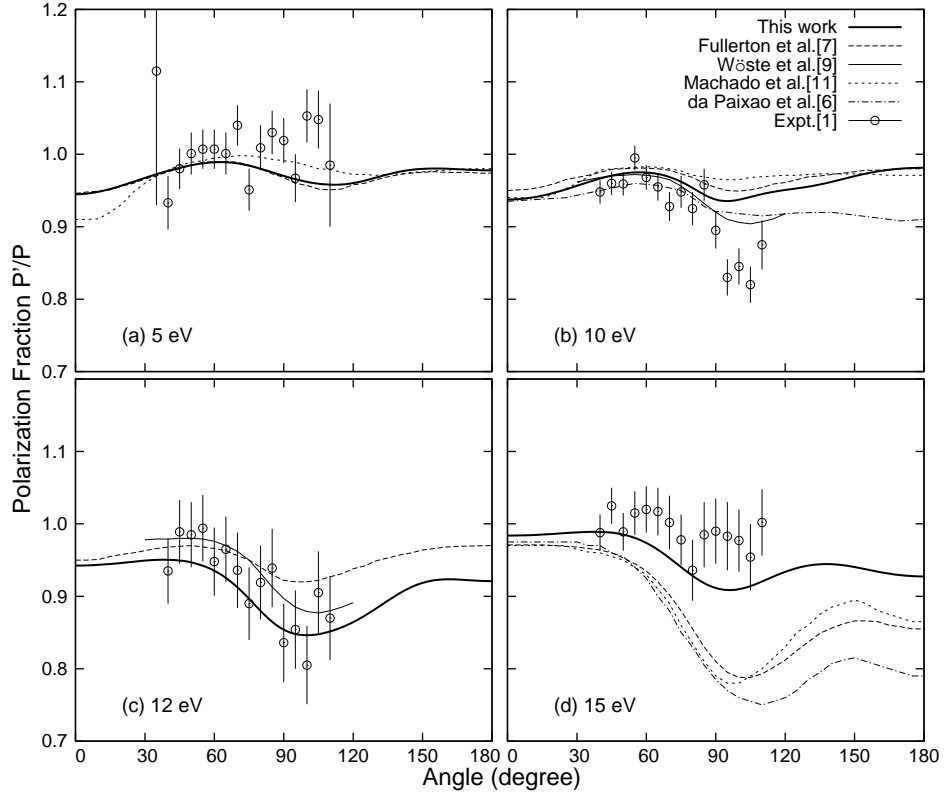


FIG. 3: Polarization fractions of electron O_2 elastic scattering. Panel (a): 5eV, (b) 10eV, (c) 12eV, (d) 15eV. Our results are shown as thick full lines. Experimental results of Hegemann et al.[1] are shown as open circles with error bars and theoretical PFs of Fullerton et al.[7], Machado et al.[11], da Paixao et al.[6], and Wöste et al.[9] are shown as thin lines.

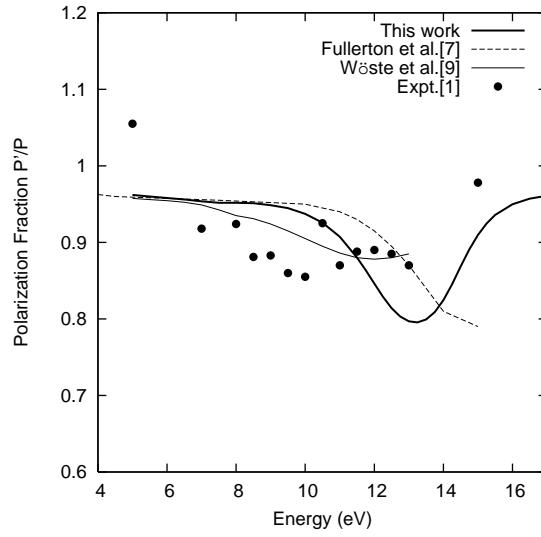


FIG. 4: Polarization fractions of electron O_2 elastic scattering, as a function of scattering energy at an scattering angle of 100 degrees. Other details are the same as in the figure 3.

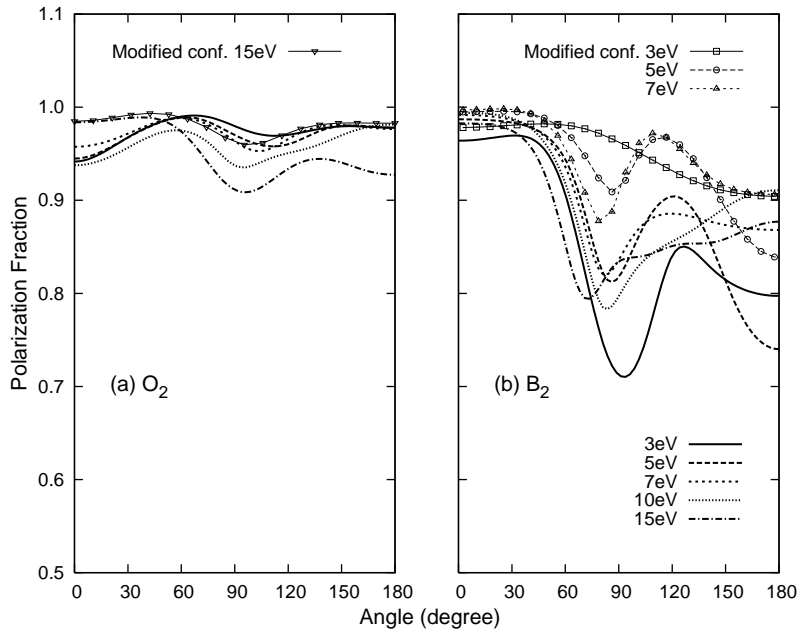


FIG. 5: Panel (a): polarization fractions (PFs) of electron O₂ elastic scattering. Panel (b): PFs of electron B₂ elastic scattering. Calculated PFs are shown as thick lines. Thin lines with symbols represent PFs without the effect of resonances, obtained by the R-matrix calculation with modified configurations (see text for details).

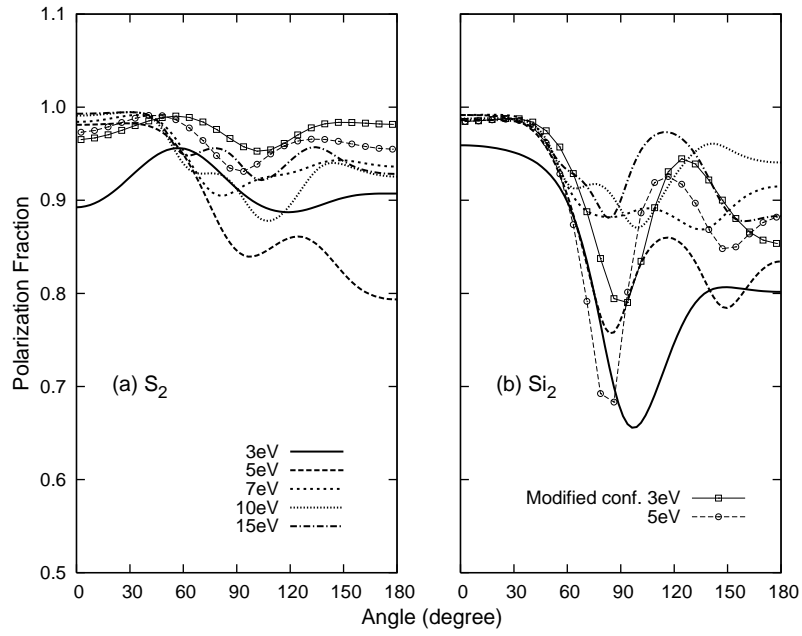


FIG. 6: Panel (a): polarization fractions (PFs) of electron S_2 elastic scattering. Panel (b): PFs of electron Si_2 elastic scattering. Other details are the same as in the figure 5.

TABLE I: List of target states included in the present R-matrix calculations.

O ₂	$X^3\Sigma_g^-, a^1\Delta_g, b^1\Sigma_g^+, c^1\Sigma_u^-, A'^3\Delta_u, A^3\Sigma_u^+, B^3\Sigma_u^-, 1^1\Delta_u, f'^1\Sigma_u^+, 1^1\Pi_g, 1^3\Pi_g, 1^1\Pi_u, 1^3\Pi_u$
B ₂	$X^3\Sigma_g^-, a^5\Sigma_u^-, b^1\Delta_g, A^3\Pi_u, c^1\Sigma_g^+, 1^3\Delta_u, 1^1\Pi_u, 1^3\Sigma_u^+, 1^3\Sigma_u^-, 1^3\Pi_g, 2^1\Sigma_g^+, 1^1\Sigma_u^-, 2^3\Pi_g, 1^1\Pi_g$
S ₂	$X^3\Sigma_g^-, a^1\Delta_g, b^1\Sigma_g^+, c^1\Sigma_u^-, A'^3\Delta_u, A^3\Sigma_u^+, B'^3\Pi_g, B^3\Sigma_u^-, 1^1\Pi_g, 1^1\Delta_u, B''^3\Pi_u, 1^1\Sigma_u^+, 1^1\Pi_u$
Si ₂	$X^3\Sigma_g^-, 1^3\Pi_u, 1^1\Delta_g, 1^1\Sigma_g^+, 1^1\Pi_u, 2^1\Sigma_g^+, 1^5\Pi_g, 1^3\Pi_g, 1^3\Sigma_u^+, 1^1\Sigma_u^-, 2^3\Pi_g, 1^3\Delta_u, 2^3\Sigma_u^+, 1^1\Pi_g, 1^3\Phi_g$

 TABLE II: Division of the orbital set in each symmetry for e-B₂ case.

Symmetry	A_g	B_{2u}	B_{3u}	B_{1g}	B_{1u}	B_{3g}	B_{2g}	A_u
Valence	1-3 a_g	1 b_{2u}	1 b_{3u}		1-3 b_{1u}	1 b_{3g}	1 b_{2g}	
Extra virtual	4 a_g	2 b_{2u}	2 b_{3u}	1 b_{1g}	4 b_{1u}	2 b_{3g}	2 b_{2g}	1 a_u
Continuum	5-43 a_g	3-23 b_{2u}	3-23 b_{3u}	2-18 b_{1g}	5-25 b_{1u}	3-20 b_{3g}	3-20 b_{2g}	2-7 a_u

TABLE III: The vertical excitation energies of the first 5 excited states for B₂ molecule, with the previous full configuration interaction (FCI) results of Hald et al.[24]. The unit of energy is eV.

State	This work	FCI
$X^3\Sigma^-$	0.00	0.00
$a^5\Sigma_u^-$	0.06	0.26
$b^1\Delta_g$	0.71	0.63
$A^3\Pi_u$	0.91	0.69
$c^1\Sigma_g^+$	0.98	0.98
$1^3\Delta_u$	1.75	1.66

TABLE IV: The vertical excitation energies of the first 5 excited states for S₂ molecule, with the previous MRD CI results of Hess et al.[25] and MRCI results of Kiljunen et al.[26]. The unit of energy is eV.

State	This work	Previous MRD CI	Previous MRCI
$X^3\Sigma^-$	0.00	0.00	0.00
$a^1\Delta_g$	0.60	0.68	0.55
$b^1\Sigma_g^+$	0.92	1.04	0.99
$c^1\Sigma_u^-$	2.77		2.45
$A'^3\Delta_u$	2.93		2.59
$A^3\Sigma_u^+$	3.03		2.58

TABLE V: The vertical excitation energies of the first 5 excited states for Si₂ molecule, with the previous MRD CI results by Peyerimhoff and Buenker [27]. The unit of energy is eV.

State	This work	Previous calculation
$X^3\Sigma^-$	0.00	0.00
$1^3\Pi_u$	0.22	0.07
$1^1\Delta_g$	0.62	0.53
$1^1\Sigma_g^+$	0.87	0.71
$1^1\Pi_u$	0.90	0.63
$2^1\Sigma_g^+$	1.44	1.14